Using Raman spectroscopy to reveal the chemical physics of water in seawater

David Jumes, Lawrence University

Mentors: Ed Peltzer, Peter Brewer, Peter Walz

Summer 2017

Keywords: Raman spectrometry, sea water, hydrogen bond enthalpy, van't Hoff equation

ABSTRACT

Raman spectroscopy is a useful technique to study hydrogen bonding in seawater. There are two species of water, hydrogen bonded and non-hydrogen bonded (free), that have noticeably different chemical properties. The hydrogen bonded species occur in multiple forms: trimers, tetramers and pentamers. These two species are in dynamic equilibrium and as temperature increases, the equilibrium shifts towards the free species. The equilibrium constant from this reaction was used to determine the hydrogen bond enthalpy (ΔH) via the van't Hoff equation. A series of van't Hoff graphs were created to determine the effects of pressure and salinity on ΔH; however, pressure and salinity had little to no effect on the enthalpy of the H-bond (pure water: $\Delta H = 2.53 \pm 0.07$ kcal/mol; sea water: $\Delta H = 2.61 \pm 0.14$ kcal/mol). I conclude that while temperature changes the ratio of hydrogen bonded to non-hydrogen bonded forms, pressure simply changes the ratio of hydrogen bonded forms within the population. Increasing pressure diminishes the proportion of the hydrogen bonded forms of greatest molecular volume.

INTRODUCTION

Water contains a network of hydrogen bonds which gives it unique chemical properties. It has low vapor pressure and a high boiling point, high heat of vaporization, surface tension and cohesion relative to its small molecular weight. In its hydrogen-bonded form, it is typically shown as a pentamer with C_2 symmetry because the free energy is minimized for this form versus other water molecule clusters (Walfaren, 1964). Some of these other forms are dimers, trimers and tetramers that are two-dimensional (Fig. 1). However, the environment's temperature, pressure and salinity may affect the intermolecular configuration of water. At deep ocean depths with high pressure and low temperature, structures that are hydrogen bonded (due to low temperature) and minimize volume (due to high pressure) are favored. It is important to note that this field has been studied extensively, and temperature has been found to have a more noticeable effect on the equilibrium between free and bound water molecules than pressure (Carey and Korenowski, 1998).

Laser Raman spectroscopy is an effective technique that can be used to characterize different chemicals based on their spectra. In this instance, we will be using it to explore how the effects of temperature, pressure and salinity change the Raman spectrum of water. It works by shining a laser in the visible spectrum onto the sample which causes an inelastic scattering of the incident light by a small number of molecules. The returning photons have a different wavelength than the incident light since a small amount of energy was used to change the vibrational energy state of the target molecules. The spectrum of water has a small, bending mode doublet peak at 1640 cm^{-1} and a much stronger water stretching mode band at 2900-3800 cm^{-1}. Previous work has been done to show that the 2900-3800 cm^{-1} band can be fit successfully to 5-Gaussian peaks with the following vibrational analyses: a second overtone of the bending mode ($2\nu_2$, 2050 cm^{-1}) and both symmetric (ν_1) and asymmetric (ν_3) stretching modes split by intermolecular coupling (ν_1^+, 3220 cm^{-1}; ν_3^+, 3390 cm^{-1}; ν_1^-, 3485 cm^{-1}; ν_3^-, 3624 cm^{-1}) (Furic et

al., 2000). It is known that intensities of the peaks change as temperature changes. For example, O-H stretching mode intensities change since more species are moving from hydrogen bonded structures to free water. However, the Raman frequency shift for these peaks remain mostly unaffected (Leonard et al., 1979). Sea water has an additional peak around 980 cm^{-1} due to the presence of sulfate, but this does not influence the overall peak shape or interfere with the water peaks studied here (Brewer et al., 2004).

One way to measure hydrogen bond strength is by relating it to the equilibrium between free and hydrogen bonded water molecules, as in

$$H_2O_{bound} \rightleftharpoons H_2O_{free}, \text{ where} = \frac{[H_2O]_{free}}{[H_2O]_{bound}}.$$

Using the van't Hoff equation, we can determine the enthalpy of the hydrogen bond:

$$\frac{dln(K)}{d(T^{-1})} = \frac{-\Delta H}{R}$$

where *K* is the equilibrium constant for the hydrogen bond to the non-hydrogen bond equilibrium in water, *T* is temperature, *ΔH* is the enthalpy of the hydrogen bond and *R* is the gas constant (Carey and Korenowski, 1998). Multiple van't Hoff graphs can be made by plotting the natural log of the equilibrium constant versus the inverse of the absolute temperature, ultimately finding ΔH. This has been explored in previous literature, where ΔH varies between 1.5-2.9 kcal/mol, depending on the solute and amount of intact versus broken hydrogen bonds within water structures (Zimmer et al., 2000). Although the vibrational modes in the water spectrum are expected to change as we alter the environment, we expect our data to also fit within this range.

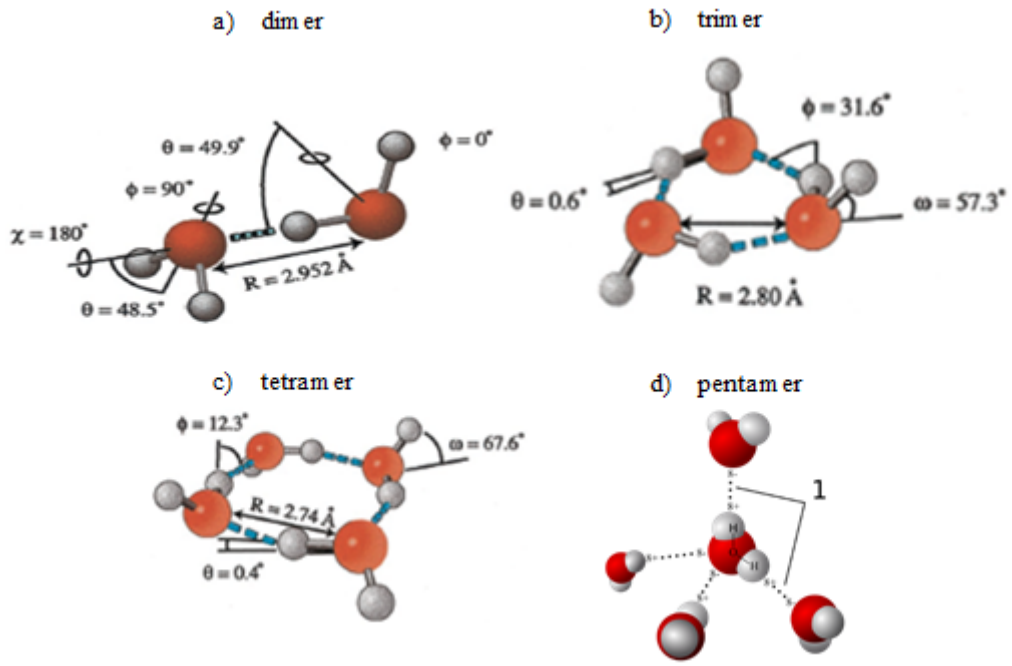

Figure 1. Various forms of hydrogen bonded water molecules. a) The dimer consists of two water molecules and one hydrogen bond. b) The trimer consists of three water molecules and three hydrogen bonds. c) The tetramer consists of four water molecules and four hydrogen bonds. d) The most common form of water, the pentamer, consists of five water molecules and four hydrogen bonds, making it three-dimensional.

MATERIALS AND METHODS

DATA COLLECTION

Data was collected using MBARI's Deep Ocean Raman In-Situ Spectrometer I (DORISS I) system (Fig. 2). A laser with a wavelength of 532 nm was emitted onto a pressure cell window constructed by Sam O. Colgate, Inc. that contained either Nanopure water or sea water collected by *Doc Ricketts* on dive V3946 (34.348 pss-78). Temperature of the pressure cell was controlled with a Thermo Scientific HAAKE DC10-K10 refrigerated circulating water bath and ranged from 0°C to 40°C with 10°C increments. Pressure was controlled by a custom-made pressure boost constructed by John Erickson at MBARI and ranged from 0 psig to 3000 psig with 500 psi increments. A total of 140 spectra were collected in duplicate using HoloGRAMS 4.1 software with an exposure time of six seconds and thirty-two accumulations. Calibrations of laser wavelength and intensity were performed with a Hololab calibration accessory to neon and white light.

DATA PROCESSING

The data were converted from Spectrum files to ASC II files and processed with a MATLAB code written by 2016 MBARI intern Matthew Wojciechowicz. A smoothing coefficient of 101 was used to remove detector noise, the baseline was corrected using pre-determined baseline points and the water spectrum from 2499.9 to 4299.9 cm^{-1} was fit to a 5-Gaussian distribution (Fig. 3). Amplitude, Raman shift, standard deviation and peak area were transcribed for each spectrum into Microsoft Excel. All further interpretations of the data and graphs were performed with Excel.

a) Complete lab set-up

b) Raman laser and pressure cell configuration

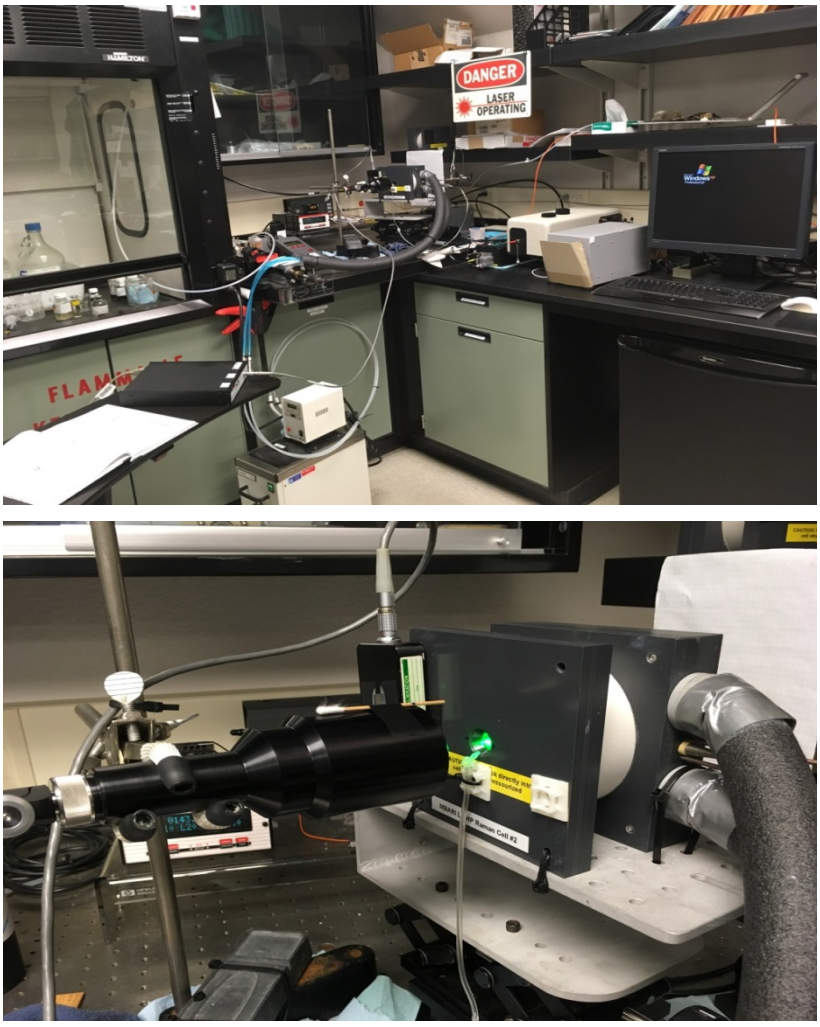

Figure 2. Laser Raman spectrometer display. a) The DORISS I system in the Brewer lab is comprised of a calibration accessory, water bath (left), pressure cell, pressure boost, laser (center) detector and optics (right). b) A close-up of the Raman laser and the pressure cell. The black box on the pressure cell is used during calibration. The airline at the bottom of the pressure cell is needed to keep condensation off the window at lower temperatures.

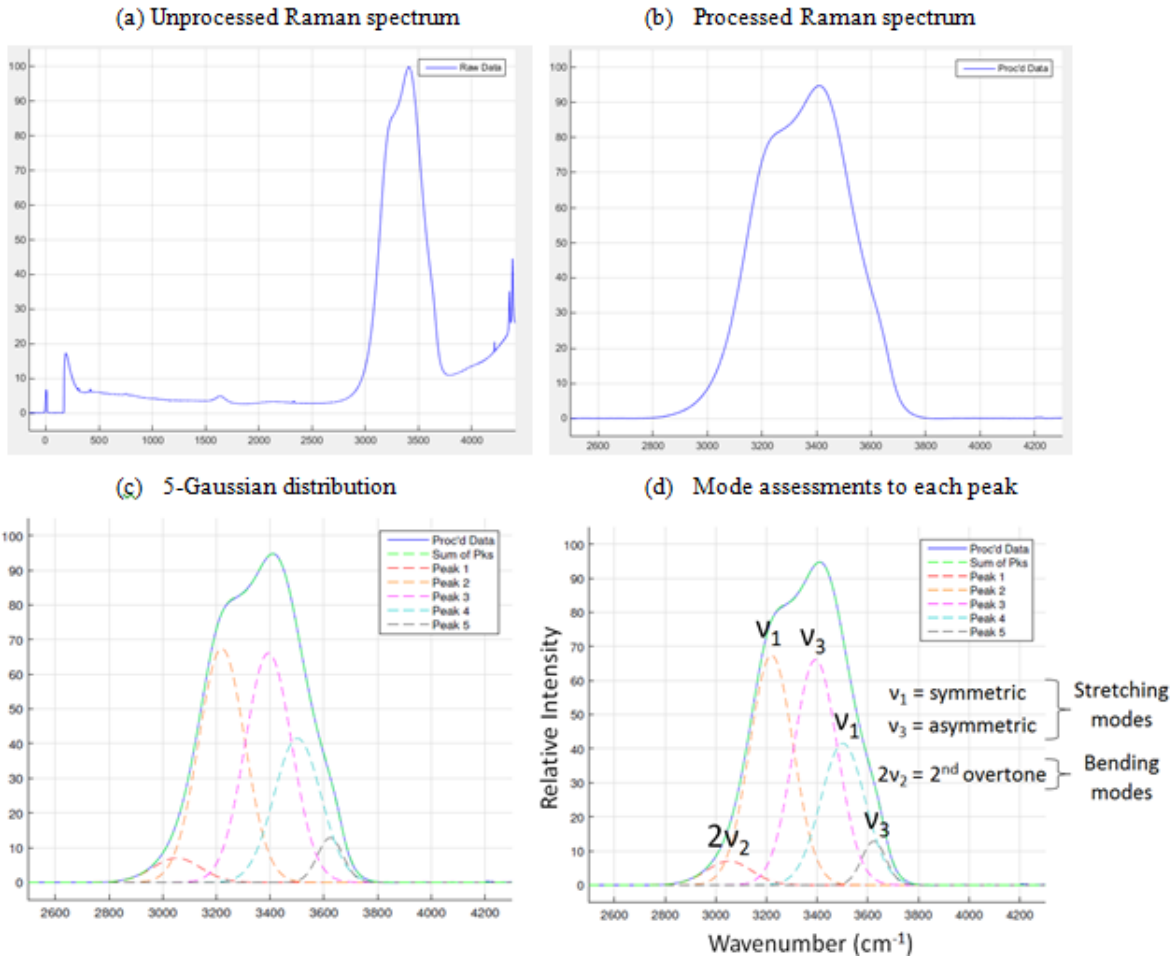

Figure 3. MATLAB analysis of the 10°C pure water spectrum at 1500 psig. a) The original spectrum as it first appeared in MATLAB. b) The processed spectrum after the x-range, smoothing coefficient and baseline was defined. c) The processed spectrum after fitting a 5-Gaussian distribution. The smoothing and fitting errors were low. d) Each peak with its corresponding stretching or bending mode.

RESULTS

RAMAN SHIFT AND RELATIVE PEAK AREA

Raman shift was unaffected by temperature, pressure and salinity (Appendix, Fig. 1). Relative peak area was affected by temperature for peaks 2, 3 and 4, whereas there was little change in area for peaks 1 and 5. Peak 2 had a negative correlation with temperature while peaks 3 and 4 had a positive correlation with temperature. Salinity and pressure had a small effect on relative peak area (Appendix, Fig. 2).

VAN'T HOFF EQUATION

Van't Hoff figures were created for each pressure and type of water (Appendix, Fig. 3). By plotting $\ln((A_3 + A_4)/A_2$ vs. T^{-1} and rearranging the van't Hoff equation, the enthalpy for hydrogen bond strength was determined. Figures of ΔH vs. pressure were constructed for each type of water to see if there was a correlation between the variables. For both water species, ΔH changed little as pressure increased and the data fit poorly to the linear regression line as seen in Figure 4 of the Appendix (pure: slope = 8×10^{-7} kcal/psig·mol, $R^2 = 0.0001$; sea: slope = 4×10^{-5} kcal/psig·mol, $R^2 = 0.0757$). The data fit well to the hypothesis that pressure has no effect on the ensemble of the hydrogen bonded species; it just changes the ratio of molecule types (trimer, tetramer, etc.). The salinity of water had little effect on ΔH, as both had similar means (pure: $\Delta H = 2.53 \pm 0.07$ kcal/mol; sea: $\Delta H = 2.61 \pm 0.14$ kcal/mol). This fit within the expected ΔH range of 1.5 – 2.9 kcal/mol for pure water (Silverstein et al., 2000). The sea water ΔH had a 5.1 % difference from previous works (Brewer et al., 2017).

DISCUSSION

Pressure and salinity had little to no effect on ΔH, as seen by the slope of both graphs and their means (Appendix, Fig. 4). However, altering these conditions may change the proportion of various hydrogen bonded forms, versus the amount of hydrogen bonds. Dimers, trimers and tetramers have little structural change as pressure increases because they are planar. Pentamers are three-dimensional and

more easily manipulated by pressure; the pentamer form is decreased as pressure increases. As mentioned in the introduction, clathrate hydrates exist in deep ocean environments with high pressure and low temperature. They can exist in structures from six to one hundred thirty-six hydrogen bonds and make up eighty-five percent of the clathrate hydrate, with the remaining fifteen percent being the encaged gas (Hester et al., 2007). Clathrates do not form in low pressure environments.

Temperature is then thought to be the determining factor in calculating ΔH, as it affects the equilibrium ratio between free and bound water. As temperature increases, the equilibrium favors free water and changes the distribution of stretching modes since more thermal energy is available. This can be seen in Figure 2 of the Appendix where the relative peak areas of peaks 2, 3 and 4 of the water spectrum change noticeably as temperature varies. Since each of these peaks correlates to a vibrational mode, we can conclude peak 2 corresponds to the symmetric stretching of the hydrogen bonded form and peaks 3 and 4 correspond to the asymmetric and symmetric non-hydrogen bonded form. Once again, the Raman spectrometer can strictly detect the bound or free form of water, not the various hydrogen bonded forms.

CONCLUSIONS/RECOMMENDATIONS

Temperature had the largest effect on the distribution of water molecules between the hydrogen of non-hydrogen bonded forms, whereas changes in salinity and pressure had little to no effect. Pressure and salinity changed the type of hydrogen-bonded water forms whereas temperature is directly altering the ratio of free versus bonded water. Unfortunately, Raman spectroscopy is incapable of determining the various types of hydrogen bonds; it can only detect the presence or absence of them.

Previous to this experiment, the pressure booster was limited to at 1500 psig. After testing, we determined it can safely reach 3000 psig (the ocean depth equivalent of roughly 2000 m); however, this is not a replacement for the

DORISS II system that operates on the ROV *Doc Ricketts*. This ROV can reach an ocean depth of 4000 m and should continue to be used for in-situ experimentation and to better understand ocean chemistry.

This work could also be used to further study the viscosity of sea water and how it affects the travel of different animals. A more viscous fluid will typically have a larger amount of hydrogen-bonded water and make animal locomotion difficult. In order for an animal to move in water, hydrogen bonds must be broken as they swim to overcome the drag of viscosity. Previous work has been done by Stanley and Batton (1969) showing that sea water has a relative higher viscosity than pure water at similar temperatures and pressures.

ACKNOWLEDGEMENTS

Thank you Ed Peltzer for introducing me to MATLAB, helping design my experiment and interpreting my results. Getting acquainted with MATLAB is no easy task and I would have been lost without him. Peter Brewer for the endless supply of books, journal articles, papers and personal insight into this field, on top of his reassurance that everything will work out when I had to switch project ideas after the cruise. Peter Walz helping set up, calibrate, use the Raman spectrometer and teach me his tricks of the trade to obtain beautiful spectra. George Matsumoto and Linda Kuhnz for their incredible job organizing the intern program and going out of their way to ensure everyone had a fun summer. The MBARI and REU interns for planning plenty of adventures outside of work. MBARI and The Packard Foundation for providing funding and making this experience possible.

References:

Brewer, P.G., Malby, G., Pasteris, J.D., White, S.N., Peltzer, E.T., Wopenka, B., Freeman, J., & Brown, M.O. (2004). Development of a laser Raman spectrometer

for deep-ocean science. Deep-Sea Research A, 51, 739-753. http://dx.doi.org/10.1016/j.dsr.2003.11.005

Brewer, P.G., Peltzer, E.T., Walz, P.M., & Wojciechowicz, M. (2017). The Speciation of Water in Sea Water and in Gelatinous Marine Animals. Marine Chemistry, http://dx.doi.org/10.1016/j.marchem.2017.05.002

Carey, D.M., & Korenowski, G.M. (1998). Measurement of the Raman spectrum of liquid water. Journal of Chemical Physics, 108, 2669-2675. http://dx.doi.org/10.1063/1.475659

Furic´, K., Ciglenec˘ki, I., & C´ osovic´,B. (2000). Raman spectroscopic study sodium chloride water solutions. Journal of Molecular Structure, 550–551, 225-234. http://dx.doi.org/10.1016/S0022-2860(00)00388-4

Hester, K.C., Dunk, R.M., White, S.N., Brewer, P.G., Peltzer, E.T., & Sloan, E.D. (2007). Gas hydrate measurements at hydrate ridge using Raman spectroscopy. Geochimica et Cosmochimica Atca, 71, 2947-2959. http://dx.doi.org/10.1016/j.gca.2007.03.032

Leonard, D.A., Caputo, B., & Hoge, F.E. (1979). Remote sensing of subsurface water temperature by Raman scattering. Applied Optics, 18,1732-1745. http://dx.doi.org/10.1364/AO.18.001732

Liu, K., Brown, M.G., Carter, C., Saykally, R.J., Gregory, J.K., & Clary, D.C. (1996). Characterization of a cage form of the water hexamer. Letters to Nature, 381, 501-502. http://dx.doi.org/10.1038/381501a0

Paull, C.K., Brewer, P.G., Ussler, W., Peltzer, E.T., Rehder, G., & Clague, D. (2003). An experiment demonstrating that marine slumping is a mechanism to transfer methane from seafloor gas-hydrate deposits into the upper ocean and atmosphere. Geo-Marine Letters, 22, 198-203, http://dx.doi.org/10.1007/s00367-002-0113-y

Silverstein, K.A.T., Haymet, A.D.J., & Dill, K.A. (2000). The Strength of Hydrogen Bonds in Liquid Water and Around Nonpolar Solutes. Journal of the American Chemical Society, 2000, 8037-8041. http://dx.doi.org/10.1021/ja000459t

Stanley, E.M., & Batten, R.C. (1969). Viscosity of Sea Water at Moderate Temperatures and Pressures. Journal of Geophysical Research, 74, 3415-3420, http://dx.doi.org/10.1029/JC074i013p03415

Walrafen, G. E. (1964). Raman Spectral Studies of Water Structure. The Journal of Chemical Physics, 40, 3249-3256. http://dx.doi.org/10.1063/1.1724992

Appendix: Figures

a) Pure water at 0 psig

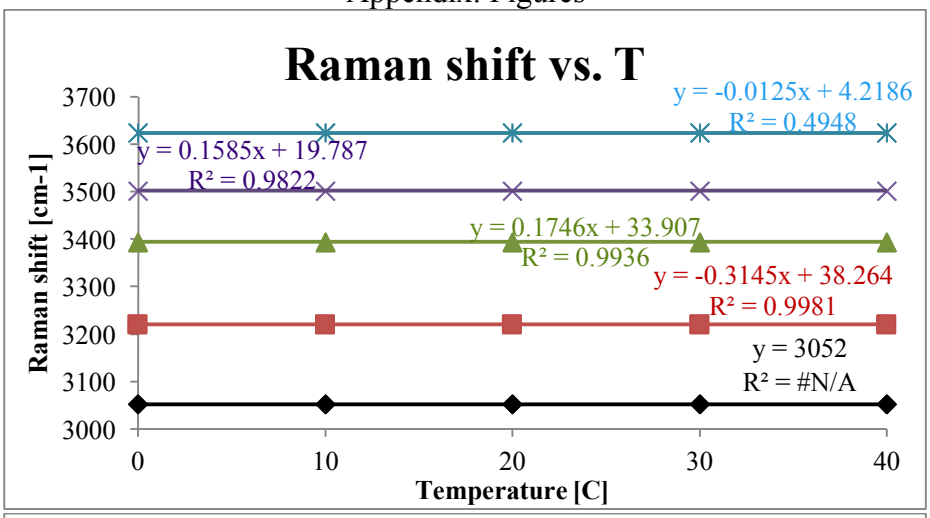

b) Pure water at 3000 psig

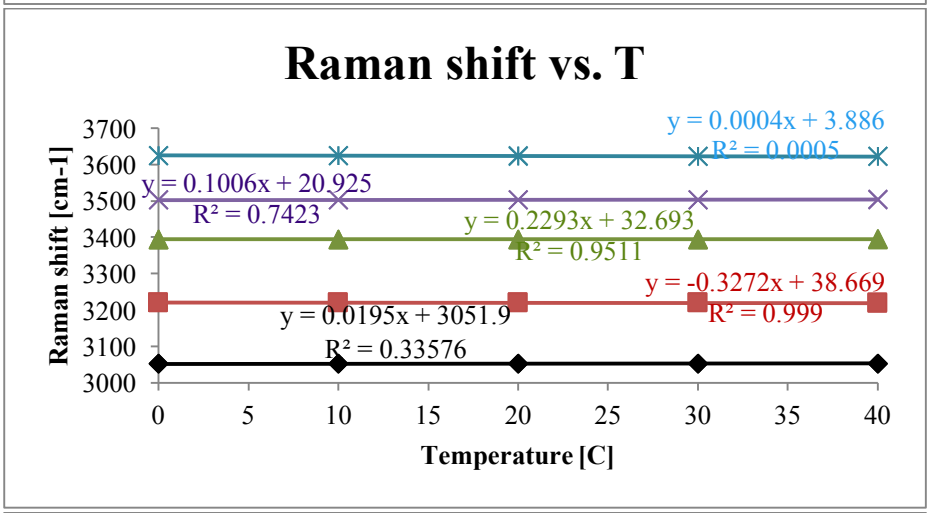

c) Sea water at 0 psig

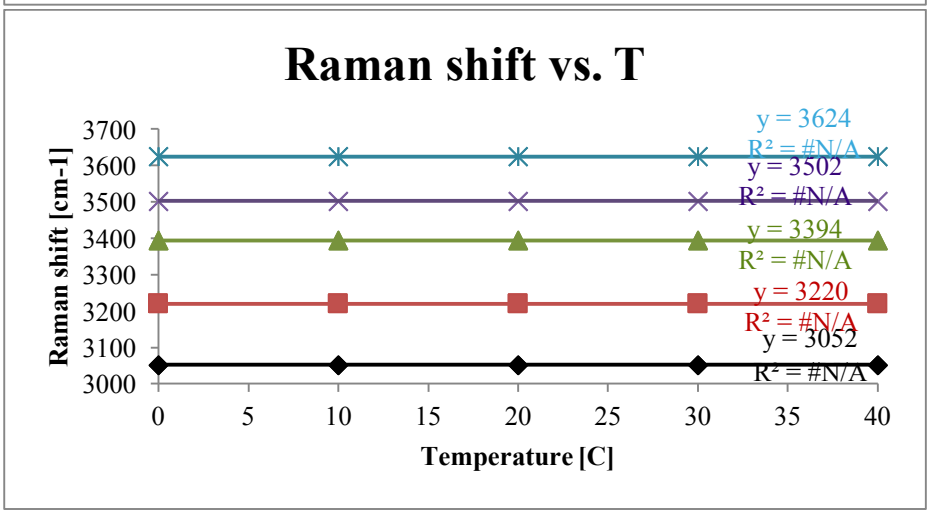

Figure 1. Raman shift versus temperature at varying pressures and salinity. Peaks 1 (black diamond), 2 (red square), 3 (green triangle), 4 (purple x) and 5 (blue x with line) are depicted above. Measurements were taken in duplicate at each temperature. Slope and R^2 values are included above the corresponding regression line. a) Pure water at 0 psig. b) Pure water at 3000 psig. c) Sea water at 0 psig.

a) Pure water at 0 psig

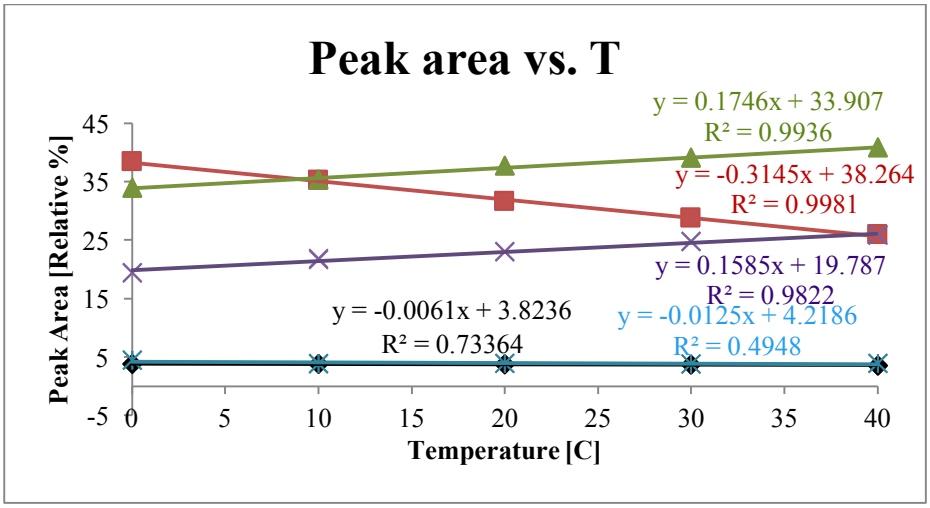

b) Pure water at 3000 psig

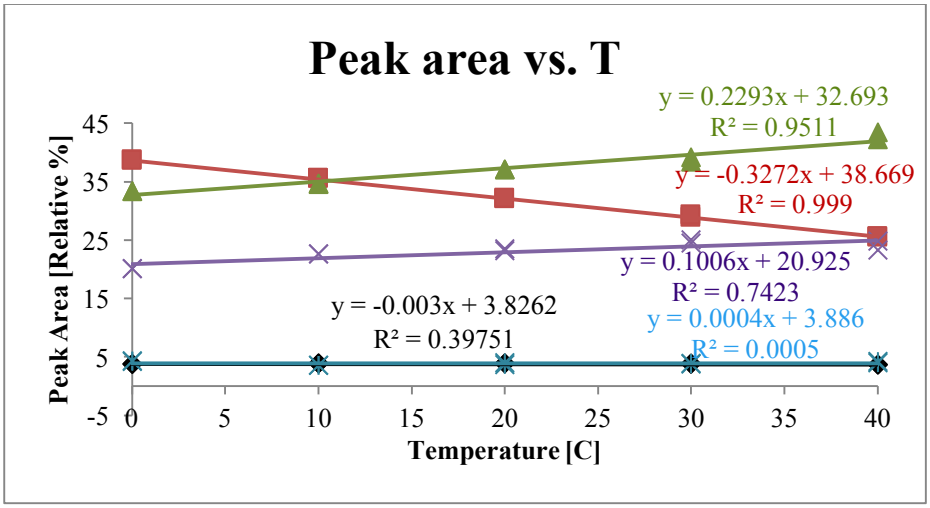

c) Sea water at 0 psig

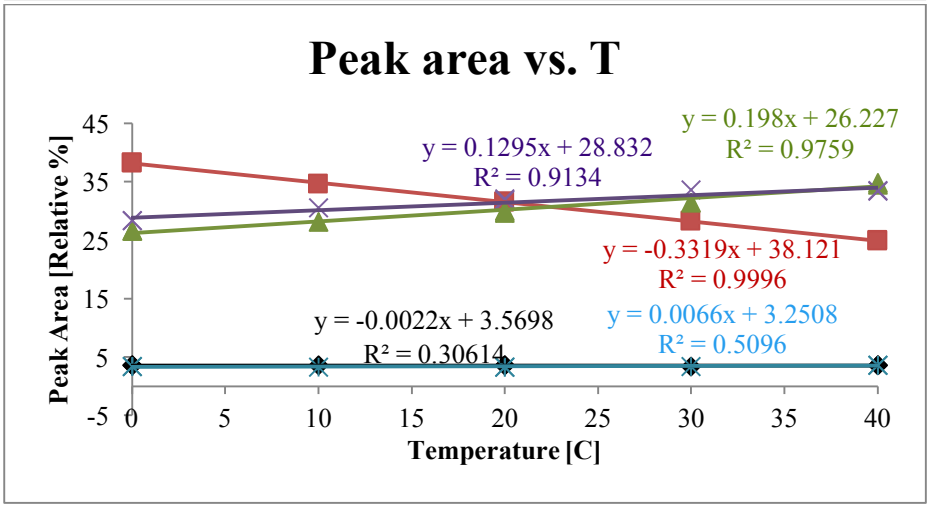

Figure 2. Relative peak area versus temperature at varying pressures and salinity. Peaks 1 (black diamond), 2 (red square), 3 (green triangle), 4 (purple x) and 5 (blue x with line) are depicted above. Measurements were taken in duplicate at each temperature. Slope and R^2 values are included above the corresponding regression line. a) Pure water at 0 psig. b) Pure water at 3000 psig. c) Sea water at 0 psig.

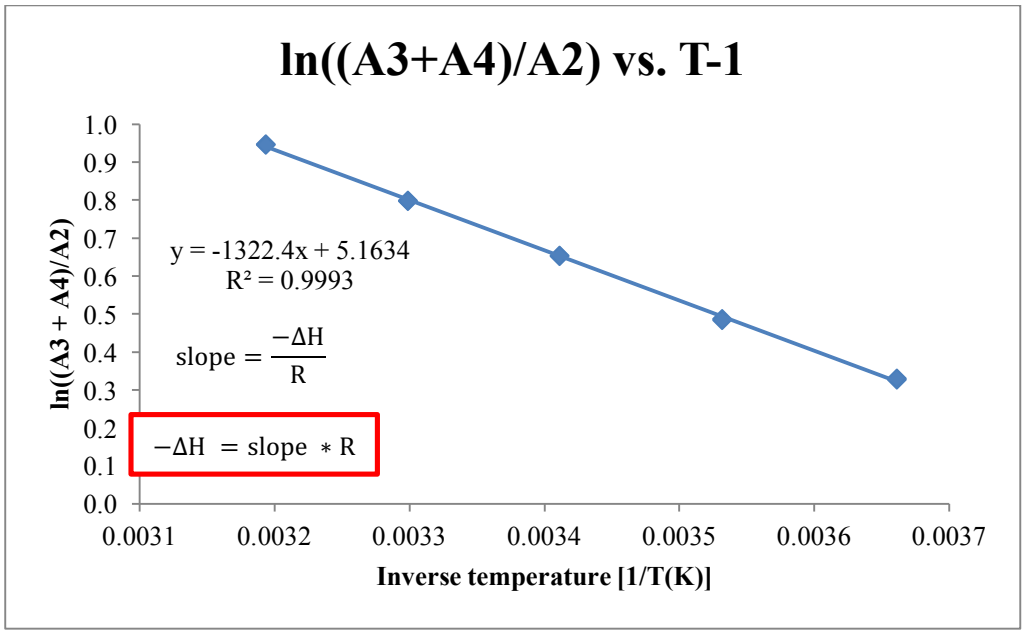

Figure 3. Van't Hoff graph of the 0 psig pure water spectrum. By plotting these variables, the enthalpy for hydrogen bond can be solved using the slope and gas constant in the van't Hoff equation. Ten data points were used and the R^2 value is close to one.

a) Pure water

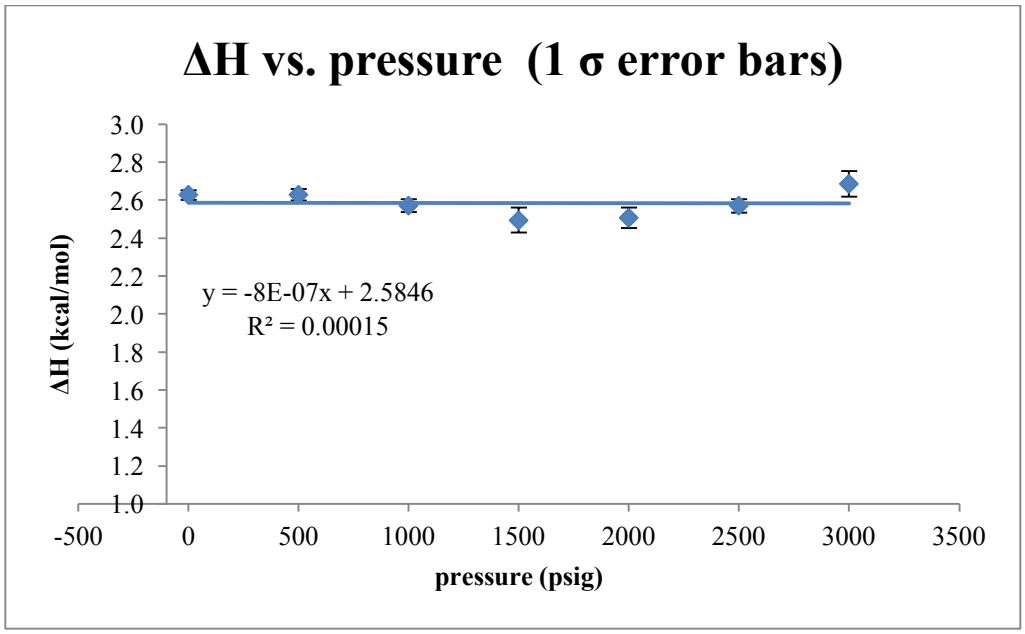

b) Sea water

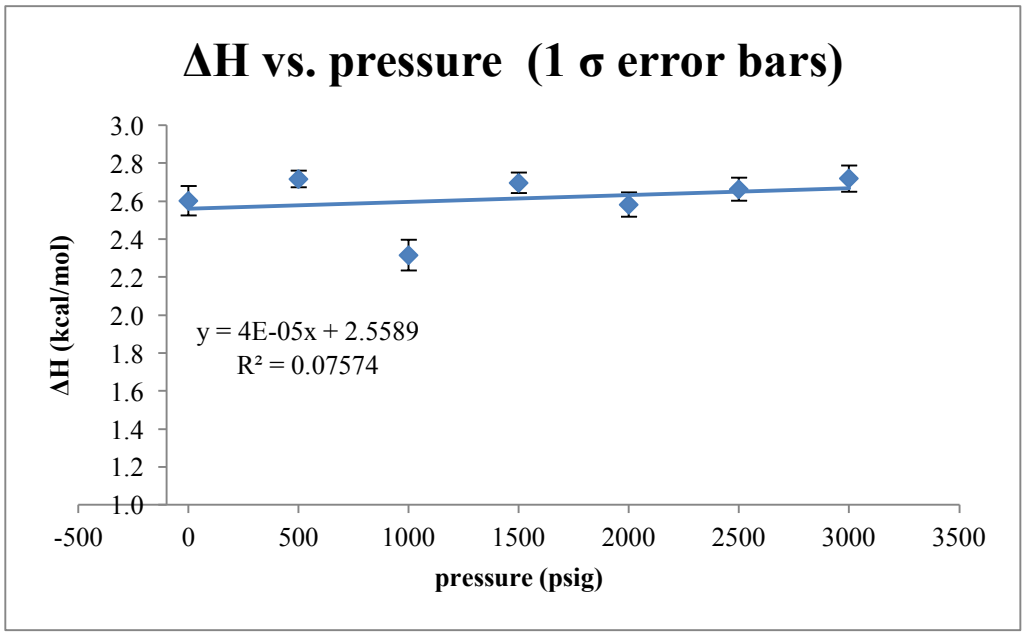

Figure 4. Relationship between ΔH and pressure. a) Pure water ΔH as pressure varies between 0 psig and 3000 psig. Error bars of 1σ are included. b) Sea water ΔH as pressure varies between 0 psig and 3000 psig. Error bars of 1σ are included.